Journal of Zhejiang University-SCIENCE A 2025 26(12):1211-1228
www.jzus.zju.edu.cn; www.springer.com/journal/11582
E-mail: jzus_a@zju.edu.cn

Research Article
https://doi.org/10.1631/jzus.A2500331

Lateral risk prediction and influencing factor analysis of container trucks based on trajectory reconstruction data

Zhihao ZHU, Hexuan LIU, Rongjun CHENG✉

Faculty of Maritime and Transportation, Ningbo University, Ningbo 315211, China

Abstract: With the continuous growth of the demand for container transportation, the proportion of container trucks passing through ports and surrounding roads has increased significantly. Due to their large size and poor maneuverability, once a truck accident occurs, it is often accompanied by serious casualties and property losses. Current research on traffic conflicts for container trucks is limited by the lack of high-quality data: first, publicly available container truck trajectory datasets are extremely rare; second, although drones have the ability to collect data over a large range, their shooting data have problems such as limited accuracy and discontinuous trajectories, which make it difficult to meet the high requirements of micro-modeling for data quality. This problem directly restricts the accuracy of conflict prediction and the credibility of causal analysis. To improve the accuracy and completeness of trajectory data, we introduce a trajectory reconstruction method to repair and complete the original trajectory. The experimental results show that the reconstructed trajectory is significantly better than the original data in terms of continuity and rationality. On this basis, a two-dimensional time to collision (2D-TTC) indicator was constructed to identify side-swipe conflict events, and based on the extraction of micro-behavior features, sample sets of side-swipe and rear-end conflicts were constructed, and a variety of machine learning models were introduced to carry out conflict prediction analysis. The results show that the gradient boosting decision tree (GBDT) model performs best in side-swipe conflict prediction, and the extreme gradient boosting (XGBoost) model in rear-end conflict prediction. By introducing the Shapley additive explanation (SHAP) method to improve the interpretability of the model, our analysis shows that the key factors influencing side-swipe conflict are the lateral speed and the average longitudinal speed within 5 s. The lateral speed reflects the lateral deviation of the vehicle, and the average longitudinal speed within 5 s reflects the driving stability and acceleration trend in a short time. The two together determine the lateral controllability of the vehicle in the dynamic process. Rear-end conflict is affected mainly by the change in longitudinal acceleration, revealing the instability of the vehicle during braking and the lack of control over the distance between the vehicle and the preceding vehicle. Finally, the model performance was optimized through feature ablation experiments, where, in the prediction of side-swipe conflicts, the GBDT achieved an accuracy of 0.911 and an area under the receiver operating characteristic curve (AUC) of 0.953.

Key words: Real-time conflict prediction; Container truck dataset; Trajectory reconstruction; Explainable machine learning; Side-swipe conflict

1 Introduction

In the area near a port, the container truck traffic flow is characterized by high density, low speed, and highly overlapping paths. Not only is the traffic organization complex, but there is also a high risk of traffic conflicts. Ordinary urban roads are dominated by intelligent connected vehicles (Li and Cheng, 2025), while the traffic subjects in a port scene are mainly heavy-loaded freight vehicles. Their poor driving stability, delayed acceleration and deceleration response, and weak control flexibility lead to traffic behaviors with significant nonlinearity and dynamic uncertainty (Ji et al., 2023). In this context, traditional data collection methods that rely on fixed sensors can no longer meet the needs of refined traffic modeling and safety assessment. In recent years, drones have become an important supplementary tool for obtaining road traffic data due to their high maneuverability and bird's-eye view. Many studies have used drones to construct high-precision trajectory datasets (Krajewski et al.,

✉ Rongjun CHENG, chengrongjun76@126.com
Rongjun CHENG, https://orcid.org/0000-0002-5558-9364

Received Jul. 19, 2025; Revision accepted Oct. 9, 2025;
Crosschecked Nov. 24, 2025

2018; Barmpounakis and Geroliminis, 2020; Zheng et al., 2024). This type of aerial observation method is particularly suitable for port areas. By shooting the container truck traffic flow, it can not only obtain the complete vehicle motion trajectory but also capture the microscopic interactions that are difficult to monitor with traditional ground equipment, laying a data foundation for subsequent more comprehensive safety analysis.

High-precision vehicle trajectory data have been widely used in the driving behavior analysis and traffic safety assessment. Many studies have used drones combined with related technologies (such as the open source computer vision library (OpenCV), Kanade–Lucas–Tomasi (KLT), and discriminative correlation filter with channel and spatial reliability (CSR-DCF)) to extract high-resolution vehicle trajectory datasets (Wang et al., 2019; Xing et al., 2020; Shawky et al., 2023). However, the trajectory data extracted using drones combined with the image recognition technology still have data accuracy problems, including vehicle type recognition errors and noises caused by some numerical differentials. These data errors not only affect the accuracy of subsequent traffic feature extraction but may also destroy the true characterization of vehicle behavior, thereby weakening the effectiveness of trajectory-based traffic safety analysis. Traditional trajectory smoothing methods mainly remove noise from trajectory data by using a moving average (Zhou et al., 2017; Gu et al., 2019; Tian et al., 2019), Savitzky-Golay filtering (Ahn et al., 2013; Zaki et al., 2014), wavelet transform (Rafati Fard et al., 2017; Hu XW et al., 2022), and other technologies to make the vehicle trajectory smoother and more continuous. However, such methods usually consider only the statistical characteristics of the data, ignoring the physical constraints and dynamic laws of vehicle motion, which can easily lead to the excessive smoothing of the trajectory and loss of real dynamic characteristics, or insufficient smoothing and residual noise (Thiemann et al., 2008). In addition, they are sensitive to parameter selection, resulting in limited applicability and versatility in different scenarios (Montanino and Punzo, 2015; Wu et al., 2019). In contrast, trajectory reconstruction methods are not only dedicated to smoothing and denoising trajectory data, but also can repair missing segments in trajectories, remove outliers, and ensure the continuity of dynamic variables such as speed and acceleration in the time dimension and the consistency of traffic behavior logic (Zhao et al., 2024a). In addition, the reconstruction process usually combines the outlier detection and trajectory interpolation technology, which is particularly suitable for data processing needs in high-noise and complex scenarios such as ports or intersections (Barmpounakis and Geroliminis, 2020; Zhao et al., 2024b). For example, some researchers proposed a 3-stage method combining wavelet transform and Savitzky-Golay filtering, which effectively improved the smoothness and coherence of intersection trajectory data (Zhao et al., 2024b); others further introduced a smoothing framework based on the Gaussian mixture and unscented Rauch–Tung–Striebel (RTS) filtering to enhance the robustness of trajectory reconstruction and its adaptability to non-Gaussian noise (He et al., 2024). Therefore, trajectory reconstruction methods have shown increasingly important research value and application potential in improving trajectory data quality and serving micro-behavior modeling and traffic safety assessment.

Due to their long bodies and large volumes, container trucks have higher requirements for surrounding space when changing lanes and merging, and their visual blind spots are significantly enlarged, which significantly increases the potential risks during lateral interactions (Jansen and Varotto, 2022; Li LY et al., 2024). In addition, trucks often travel at lower speeds in specific scenarios, such as port areas, which often prompt small vehicles behind to frequently change lanes and overtake to improve traffic efficiency, further exacerbating the lateral interference of traffic flow. In such complex traffic environments, lane changes are particularly frequent, and interactions between lanes are complex. Side-swipe conflicts have become a common but underestimated high-risk event (Chen et al., 2020; Ouyang et al., 2025). At present, mainstream traffic conflict research focuses on longitudinal conflict types, especially rear-end conflicts. Identification and warning methods generally adopt longitudinal safety indicators such as time to collision (TTC) (Xing et al., 2019; Orsini et al., 2021; Hu YP et al., 2022). Such methods are usually based on the following assumptions: vehicles are in the same lane, the longitudinal approach is the main source of risk, and conflict judgment depends on changes in speed and distance. However, in real traffic scenarios, especially complex sections involving frequent lane changes or

lane merging, this 1D longitudinal assumption may not accurately reflect the way in which lateral risks are generated (Hou et al., 2024). Some improved methods, such as time to collision with disturbance (TTCD), have introduced longitudinal speed fluctuation factors (Xie et al., 2019). The anticipated collision time (ACT) indicator was further expanded into a two-dimensional time to collision (2D-TTC) in a study to simultaneously characterize the lateral and longitudinal relative motion characteristics. This indicator was successfully used to identify multiple types of conflicts, including side collisions (Venthuruthiyil and Chunchu, 2022). In terms of risk modeling, some recent studies have begun to attempt to identify potential conflicts in the 2D trajectory space. For example, one study proposed a 2D collision detection method based on intersection trajectory analysis to identify high-risk events in lane changes and cross paths in advance (Ward et al., 2015). Another study developed an analytical algorithm for calculating lateral TTC and theoretically modeled lateral conflicts under idealized trajectory reconstruction conditions (Hou et al., 2014). However, these methods still face some serious problems in practical applications: first, most studies rely on high-precision sensors or simulation data, which makes it difficult to meet the real-time application requirements of large-scale, natural scenes (Hu YP et al., 2022); second, in truck traffic flows involving large vehicles, high response lag, and weak control flexibility, the robustness and adaptability of existing models still need to be improved (Li et al., 2022; Tian et al., 2024).

Traffic conflict prediction generally adopts data-driven methods, and the mainstream methods mostly adopt a binary classification framework, that is, to identify whether a conflict occurs. Among them, the machine learning has been widely used in conflict detection and risk assessment tasks due to its excellent prediction performance (Katrakazas et al., 2018; Li et al., 2020; Mohammadian et al., 2021; Yuan et al., 2022). Compared with traditional statistical methods, the machine learning and deep learning have significant advantages, especially in dealing with complex nonlinear relationships and high-dimensional features (Yao et al., 2021; Islam and Abdel-Aty, 2023). In recent years, researchers have also proposed a variety of methods to further improve the model performance and adaptability. Some scholars developed a non-parametric model based on machine learning for conflict prediction at signalized intersections, and improved the accuracy and transferability of the model through Bayesian optimization (Zheng et al., 2023); others have proposed a unified probabilistic modeling method that regards traffic conflicts as extreme events in interactions, thereby achieving effective detection of multiple environments and types of conflicts (Jiao et al., 2025). However, despite the continuous improvement in model performance, most of these methods are still "black box models" and it is difficult to explain how the features specifically affect the prediction results. This limitation restricts their application in traffic safety analysis and policy making. To enhance the interpretability of the model, local interpretation methods (such as the local interpretable model-agnostic explanations (LIME) and Shapley additive explanation (SHAP)) have been gradually introduced in recent years. The LIME approximates the behavior of complex models near a single point by constructing a local linear model, and the calculation is relatively simple (Ribeiro et al., 2016), while SHAP is based on the Shapley value principle and measures the contribution of each feature to the model output from a game theory perspective, which is suitable for local and global interpretations (Lundberg and Lee, 2017). Studies have shown that SHAP can provide stable and consistent interpretation results in traffic risk identification. Some studies have used categorical boosting (CatBoost) and SHAP frameworks to identify key factors affecting highway safety (Li JQ et al., 2024). Others have compared the differences in risk characteristics of different types of drivers (Peng et al., 2024). These studies show that interpretability methods are of great significance in improving model transparency and policy application value.

This paper focuses on the traffic flow around a port, which is composed mainly of container trucks, and conducts the real-time traffic safety analysis around side-swipe and rear-end conflicts. The original trajectory data are reconstructed to improve data accuracy and be more in line with physical laws. On this basis, a 2D-TTC indicator is developed based on the coordinate format output by you only look once, version 8 (YOLOv8) to realize the identification of side-swipe conflicts. At the same time, rear-end conflict data are collected to construct a sample set containing two types of conflict events. Subsequently, a variety of machine learning models are constructed to predict and model

side-swipe conflicts and rear-end conflicts, and the performance of the models under different feature combinations is compared. Then, combined with the SHAP interpretability method, the role mechanism of each influencing factor in different conflict types is deeply analyzed. The best performing model based on preliminary analysis is further improved through feature superposition experiments. The main contributions of this paper include the following:

(1) The trajectory reconstruction process was performed on a traffic flow trajectory dataset consisting mainly of container trucks, and a high-precision dataset that complies with physical laws was obtained.

(2) A TTC index based on 2D space is proposed to identify and extract side-swipe conflict samples, which solves the problem of insufficient side-swipe conflict recognition of traditional TTC methods.

(3) A variety of machine learning models were used to model and predict the two types of typical conflicts. Through different feature combinations and feature ablation experiments, a model with better prediction performance was obtained, which will play an important role in future intelligent truck loading conflict prediction modules.

(4) The SHAP theory was used to conduct an interpretable analysis of the model results, and the specific impact of various characteristics on the two types of conflicts was deeply explored.

This paper is organized as follows: Section 2 introduces the methods involved in this study; Section 3 presents the results of trajectory reconstruction and conflict prediction modeling and conducts a preliminary analysis; Section 4 provides a discussion, analyzing in detail the specific impact of features on these two conflict types and pointing out the shortcomings of this study; Section 5 summarizes the entire paper.

2 Methodology

First, the original trajectory data are reconstructed to ensure the quality and rationality of the trajectory data. Then, 2D-TTC and TTC are used to identify the side-swipe and rear-end conflicts in the reconstructed data. On this basis, the feature extraction is performed to complete the construction of the conflict sample, thus completing the sample production process. The samples are divided into training sets and test sets. The training set is used to train the machine learning model. The model with the best prediction performance is obtained through evaluation indicators to predict whether a conflict will occur. Then, the SHAP theory is used to analyze how each factor specifically affects the occurrence of conflict. Finally, according to the order of feature importance, the features are superimposed in sequence to perform feature ablation experiments to further improve the prediction performance of the model. The overall method framework is shown in Fig. 1.

2.1 Trajectory reconstruction

The video dataset was shot in windless and sunny weather, and abnormal videos were removed. All videos were anti-shake processed, but may still have data quality issues. Therefore, it was necessary to reconstruct the trajectory data extracted by YOLOv8. The method of trajectory reconstruction is based on a

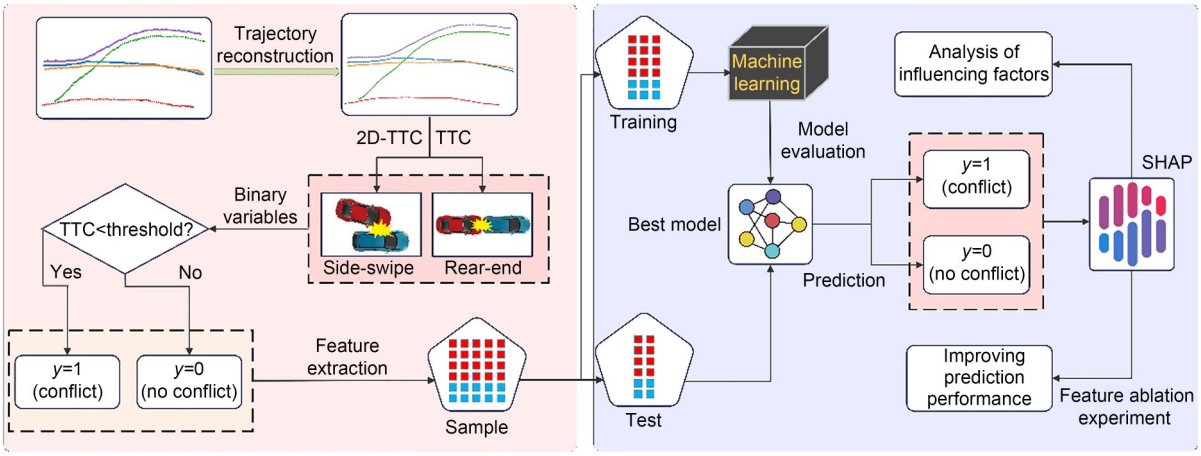

Fig. 1 Method framework diagram

previous study (Zhao et al., 2024a), but due to the inclusion of different scenarios, the method is changed.

2.1.1 Objective function

The Euclidean distance is used to measure the deviation between the reconstructed trajectory and the original trajectory (Fig. 2). The trajectory reconstruction problem is transformed into a nonlinear optimization problem, and the optimization goal is to minimize the root mean square error (RMSE) value of the reconstructed trajectory and the original trajectory. The objective function can be expressed by the following equation:

$$C_{\min}=\min\sqrt{\frac{1}{N}\sum_{i=1}^{N}D(L_i)}, \tag{1}$$

where C is the cost function of reconstructing the trajectory, L_i is the coordinate information of each sampling point, i is the index of the sampling point, N is the number of sampling points in each trajectory, and $D(L_i)$ is the cost of reconstructing the ith sampling point of a single trajectory, which can be calculated by Eq. (2).

$$D(L_i)=(X_i-X_{\text{orignal},i})^2+(Y_i-Y_{\text{orignal},i})^2, \tag{2}$$

where X_i and Y_i are the position coordinates of the ith reconstructed trajectory point, $X_{\text{orignal},i}$ and $Y_{\text{orignal},i}$ are the position coordinates of the ith original trajectory point, and the unit of the coordinates is m.

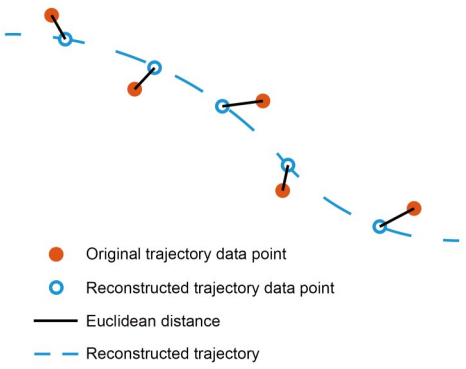

Fig. 2 Trajectory reconstruction principle

2.1.2 Constraints

The reconstructed trajectory needs to conform to objective laws, so the speed, acceleration, and rate of change of acceleration should be limited within a reasonable range according to the traffic rules and vehicle characteristics of the study area. At the same time, different vehicles have different characteristics, and the range of restrictions should also be different. The given constraints are as follows:

(1) Speed constraint. Vehicles in the study area travel in one direction, so the speed (v) must be greater than or equal to 0, and the maximum speed normally does not exceed the speed limit of the road section.

$$0\leqslant v\leqslant v_{\max}, \tag{3}$$

where $v_{\max}$ is set to 23 m/s.

(2) Acceleration constraints. The vehicles in the study area can be divided into two main types: container trucks and cars. The characteristics of these two vehicles are different. Container trucks usually have slower acceleration than cars, so there are different constraints on these two types of vehicles.

$$a_{\text{Tmin}}\leqslant a_{\text{T}}\leqslant a_{\text{Tmax}},\quad a_{\text{Cmin}}\leqslant a_{\text{C}}\leqslant a_{\text{Cmax}}, \tag{4}$$

where a_{T} represents the acceleration of the truck and a_{C} is the acceleration of the car. The acceleration range of the truck is limited to between −3 and 3 m/s^2, and the acceleration range of the car is limited to between −5 and 5 m/s^2 (Liu et al., 2022).

(3) Acceleration rate constraint (jerk constraint). Jerk is the first-order derivative of acceleration with respect to time, which measures the change in acceleration per unit time. In human–vehicle interaction applications, it is an important variable used to evaluate comfort.

$$-j_{\max}\leqslant\frac{a(k+1)-a(k)}{\Delta t}\leqslant j_{\max}, \tag{5}$$

where $j_{\max}$ is the maximum value of the rate of change of acceleration (a), which is set to 10 m/s^3 (Martinez and Canudas-de-Wit, 2007), k represents the time index, and Δt represents the time interval, which is 0.1 s here.

2.1.3 Solution

The trajectory reconstruction problem is transformed into a nonlinear optimization problem using the above formula. Python language is used for programming, and the interior point optimizer (IPOPT)

algorithm in the numerical optimization toolbox CasADi is used for solving (Wächter and Biegler, 2006; Andersson et al., 2019).

This experiment is carried out on multiple servers equipped with a 12 vCPU Intel(R) Xeon(R) Silver 4214R 2.40 GHz processor, an NVIDIA RTX 3080 Ti (12 GB) GPU, and 90 GB of memory. The convergence condition is that the change in the objective function value is less than a certain threshold, which is set to 1×10^{-6}.

2.2 Conflict identification

This study used characteristic thresholds to distinguish between conflict and non-conflict scenarios. Not all interactions were considered conflicts. A more detailed distinction was made between rear-end conflicts and side-swipe conflicts. A rear-end conflict was considered a conflict if its magnitude was below a certain threshold, while a side-swipe conflict was considered a conflict only if it satisfied Eq. (11) and was below a certain threshold.

2.2.1 Rear-end conflict

This study used TTC (Hayward, 1972) to identify rear-end conflicts. The TTC (T) can be calculated by the following equation:

$$T=\begin{cases}\dfrac{g_x}{v_\mathrm{r}-v_\mathrm{f}}, & v_\mathrm{r}\neq v_\mathrm{f},\\ +\infty, & v_\mathrm{r}=v_\mathrm{f},\end{cases} \tag{6}$$

where g_x is the distance between the front and rear vehicles in the X direction, v_r is the speed of the rear vehicle, and v_f is the speed of the front vehicle.

2.2.2 Side-swipe conflict

For side-swipe conflicts, a 2D-TTC was developed based on TTC and combined with the coordinate characteristics of the YOLOv8 detection box to identify side-swipe conflicts. The specific principle is shown in Fig. 3. First, some implicit conditions for side-slip collisions must be clarified. The longitudinal speed of the rear vehicle must be greater than that of the front vehicle; otherwise, there will be no collision. Then, the interaction between the front and rear vehicles in the 2D direction is considered, and finally, two extreme situations where collisions may occur are obtained (Figs. 3b and 3c).

The coordinates (X_c and Y_c) of the collision point can be calculated by Eq. (7). The TTCs in the longitudinal direction of the two extreme cases are different and can be calculated by Eqs. (8) and (9). The lateral TTC can be calculated according to Eq. (10). If the lateral TTC is between the longitudinal TTCs of these two cases, it is considered that conflict is likely to occur, which can be expressed by Eq. (11).

$$\begin{cases}X_\mathrm{c}=X_\mathrm{f\text{-}lr}-W_\mathrm{f}\sin\theta,\\ Y_\mathrm{c}=Y_\mathrm{f\text{-}lr},\end{cases} \tag{7}$$

where ($X_\mathrm{f\text{-}lr}$, $Y_\mathrm{f\text{-}lr}$) is the coordinate of the lower right corner of the front vehicle detection box, W_f is the

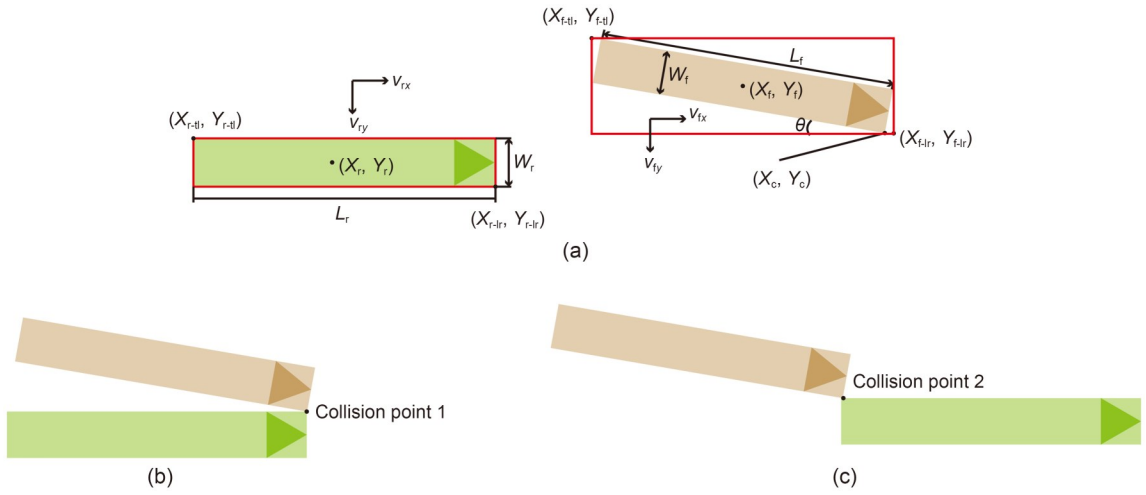

Fig. 3 Side-swipe conflict identification principle: (a) precursor of side-swipe conflict; (b) extreme case 1 of side-swipe conflict; (c) extreme case 2 of side-swipe conflict

width of the front vehicle, and θ is the heading angle of the vehicle.

$$T_{x_1}=\frac{X_{\mathrm{c}}-X_{\mathrm{r\text{-}lr}}}{v_{\mathrm{rx}}-v_{\mathrm{fx}}}, \tag{8}$$

$$T_{x_2}=\frac{X_{\mathrm{c}}-X_{\mathrm{r\text{-}lr}}+L_{\mathrm{r}}}{v_{\mathrm{rx}}-v_{\mathrm{fx}}}, \tag{9}$$

where $X_{\mathrm{r\text{-}lr}}$ is the X coordinate of the lower right corner of the rear vehicle detection box, L_{r} is the length of the rear vehicle, and v_{rx} and v_{fx} are the longitudinal speeds of the rear vehicle and the front vehicle, respectively.

$$T_y=\frac{Y_{\mathrm{r\text{-}tl}}-Y_{\mathrm{c}}}{v_{\mathrm{fy}}-v_{\mathrm{ry}}}, \tag{10}$$

$$T_{x_1}\leqslant T_y\leqslant T_{x_2}, \tag{11}$$

where $Y_{\mathrm{r\text{-}tl}}$ is the Y coordinate of the top left corner of the rear vehicle detection box, and v_{fy} and v_{ry} are the lateral speeds of the front and rear vehicles, respectively.

2.3 Conflict analysis

2.3.1 Conflict prediction

Traffic conflict prediction is essentially a binary classification problem. Machine learning models are well-suited for solving this problem. In this study, we trained multiple machine learning models for traffic conflict prediction. Logistic regression (LR) (Safavian and Landgrebe, 1991) maps input features to probability values through a logical function and is suitable for simple binary classification problems. Support vector machines (SVMs) (Vapnik, 1995) maximize class intervals by finding the optimal hyperplane and are particularly suitable for high-dimensional data. Extreme gradient boosting (XGBoost) (Chen and Guestrin, 2016) is an efficient gradient boosting framework that gradually improves model performance by iteratively optimizing weak learners. Gradient boosting decision tree (GBDT) (Friedman, 2001) gradually improves the overall prediction performance by iteratively training multiple decision trees to fit the residuals and is suitable for dealing with nonlinear relationships and feature interaction problems.

2.3.2 Model evaluation

We used five criteria to evaluate model performance. The first three criteria were accuracy (ACC), false negative rate (FNR), and false positive rate (FPR). These indicators were based on the confusion matrix and calculated using Eqs. (S1)–(S3) in Section S1 of the electronic supplementary materials (ESM). The higher the ACC value, the better the model performance. And lower FNR and FPR values indicate better model performance. In addition, the receiver operating characteristic (ROC) curve and the area under the curve (AUC) were used as evaluation metrics (Bradley, 1997). The ROC curve illustrates the relationship between the true positive rate (TPR) and the FPR across different decision thresholds. TPR can be calculated using Eq. (S4). The AUC value ranges from 0 to 1: the closer to 1, the better the model performance.

2.3.3 SHAP

SHAP has been widely used to explain machine learning models (Islam and Abdel-Aty, 2023). Based on Shapley values from game theory, it assigns feature contributions in a consistent and equitable manner. By quantifying each feature's marginal contribution across different combinations, SHAP provides interpretable explanations of model outputs. A positive or negative SHAP value indicates that the feature has a positive or negative impact on the prediction. In this study, we used SHAP to analyze how features affect conflicts. The detailed principle of SHAP can be found in Eqs. (S5)–(S7) of the ESM.

3 Data and results

3.1 Data preparation

This dataset is a collection of high-definition images of vehicles on the road section of Meishan Island, Ningbo, China, taken by drones. The total video length is about 40 h, the resolution is 1920×1080 pixels, and the frame rate is 30 f/s. The dataset contains vehicle images at different time periods, all taken in windless and clear or light wind conditions, with high resolution and real scene characteristics. Since Meishan Island is an important port and logistics center, almost 80%–90% of the vehicles on the road are container trucks, and the traffic flow properties are special.

First, the video dataset was subjected to abnormal video removal and anti-shake processing, and then the vehicle trajectory was extracted using YOLOv8 (Fig. 4). The vehicle position was recorded using the

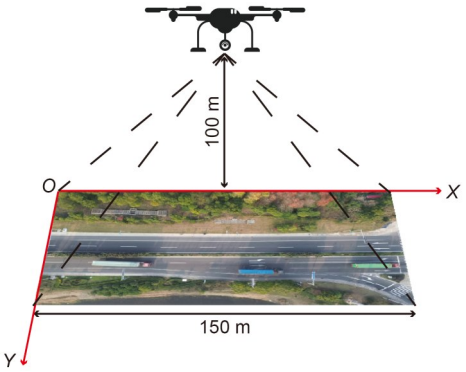

Fig. 4 Road section recorded by drone

global coordinate system. The origin of the coordinate was set at the upper left corner of the road section. The *X* coordinate increased as it moved to the right, and the *Y* coordinate increased as it moved down the road. The initially extracted trajectory data included the frame number, ID, type of target vehicle, center coordinates of the target vehicle and their respective lengths and widths, coordinates of the upper left and lower right corners of the target vehicle detection frame, and other calculated data (Section S2 of the ESM). Details of the dataset construction process can be found in a previous article (Zhu et al., 2025).

3.2 Trajectory reconstruction effect

After eliminating abnormal trajectories, a total of 24038 trajectories were reconstructed. The reconstructed trajectories of some vehicles are shown in Fig. 5. Figs. 5a and 5c are the complete trajectories of a vehicle changing lanes to the right. The vehicle in Fig. 5a changes one lane, and the vehicle in Fig. 5c changes two lanes. Fig. 5b shows the trajectory of a vehicle driving to the right into the right-turn lane.

Although the trajectories of Figs. 5d–5f seem to fluctuate greatly, the ordinate indicates that they were in a straight-line state, and the overall fluctuation is consistent with the actual driving situation. Although the reconstructed trajectory is relatively close to the original trajectory, the zoom data show that the data points of the original trajectory are jagged and there is some obvious noise, while the reconstructed trajectory is a relatively smooth path.

Fig. 6 shows the Euclidean distances between the reconstructed trajectory data points and the original data points. The Euclidean distances for most data points were relatively large, indicating that the reconstructed trajectory differs significantly from the original trajectory. However, Fig. 5 shows that the differences between the data points in the *Y* direction are not very large, and theoretically, a large Euclidean distance should not result. Looking at the *X* direction, the reconstruction reveals that the data point at the end of the original trajectory has shifted to the left, which is likely a reasonable phenomenon. Drones are affected by wind when collecting video data. Although shooting in clear, calm weather is recommended, they can still be affected. Drones are easily affected in the *X* direction, resulting in some unreasonable data points in this direction, such as excessive longitudinal displacement between data points. This explains the large Euclidean distances between the data points in Fig. 6.

Section S3 of the ESM shows the comparison of speed and acceleration in 2D space before and after reconstruction, as well as the comparison of jerk. The data of the original trajectory are largely inconsistent with the actual situation, while the data of the reconstructed trajectory have been greatly improved and are more consistent with the actual situation.

To ensure the rationality of the reconstruction results, we merged all trajectory dataset files and plotted longitudinal and lateral velocity and acceleration histograms to verify the accuracy of the trajectory reconstruction (Fig. 7). The longitudinal velocity was concentrated between 0 and 5 m/s, peaking at 0 m/s, reflecting frequent vehicle stops and starts. The longitudinal acceleration was centered around 0 m/s^2, with slightly more negative values, consistent with deceleration, yielding, and starting. Both the values of lateral velocity and acceleration were concentrated near 0, indicating no significant lane changes or turns, and minimal lateral movement, which was consistent with the vehicle approaching an intersection but not entering it. The overall distribution was reasonable and consistent with the dataset's collection scenario (i.e., a road section near an intersection).

3.3 Analysis of factors affecting conflict

The conflict samples were extracted from the reconstructed trajectory data. A TTC value of 3 s was finally selected as the threshold for distinguishing conflicts, based on literature (Shahana and Vedagiri, 2024). Finally, 1506 rear-end conflicts and 264 side-swipe conflicts were extracted (Table 1). The selection of relevant features retained the speed and acceleration

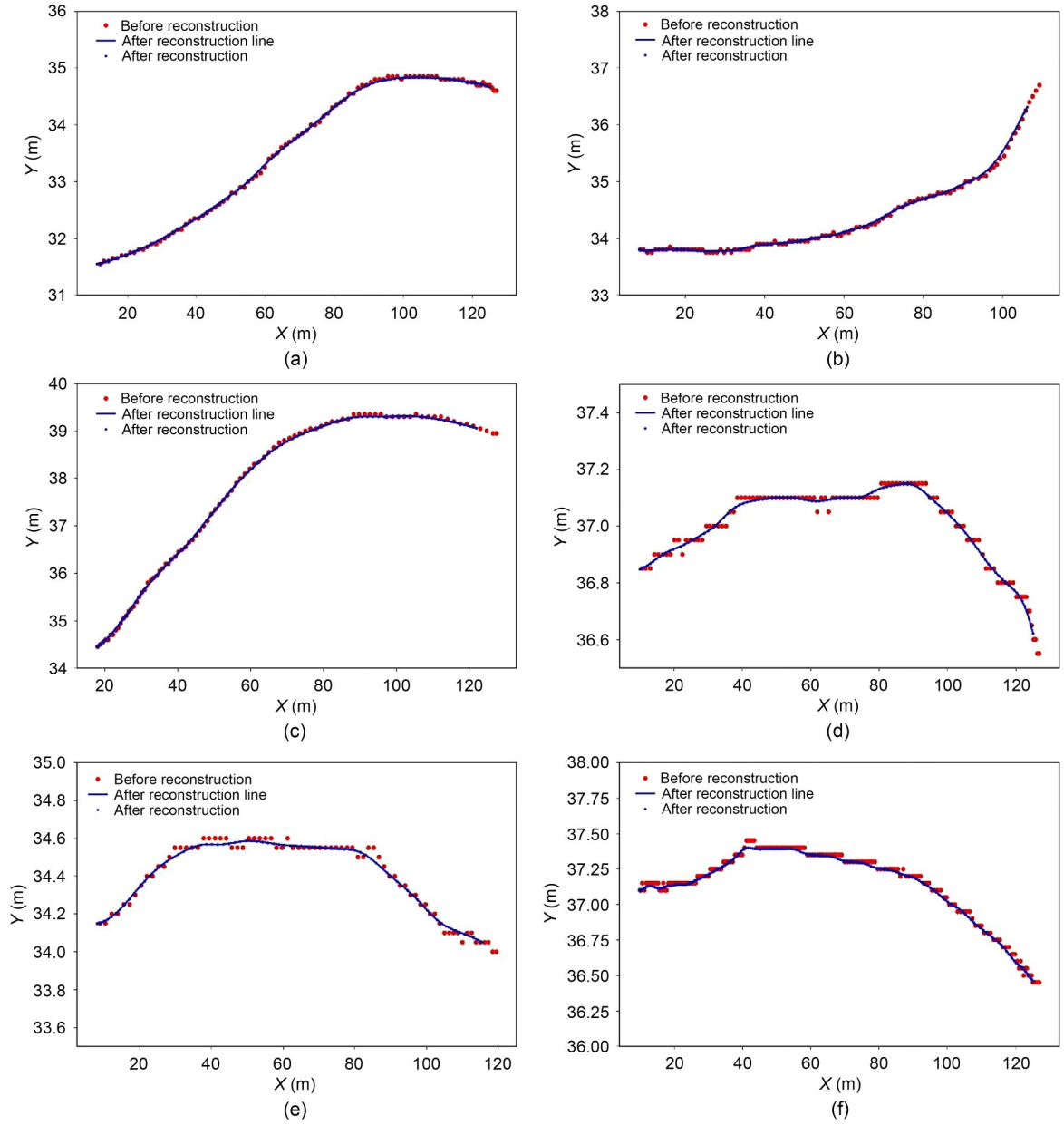

Fig. 5 Comparison of trajectories before and after reconstruction: (a) trajectory ID 752; (b) trajectory ID 356; (c) trajectory ID 139; (d) trajectory ID 39; (e) trajectory ID 251; (f) trajectory ID 297. References to color refer to the online version of this figure

features, as well as the calculated heading angle, and the mean and standard deviation (SD) of these features. The calculation ranges of the mean and SD were selected to be within 5 s. The statistical description of the relevant variables is shown in Sections S4 and S5 of the ESM.

The two types of conflict samples were trained separately: 80% of the sample data were used as the training set, 20% as the test set, and five-fold cross-validation was used to make full use of the data. The selected classification models were SVM, LR, XGBoost, and GBDT. To select the model with the best performance, a cross-grid was used to find the best parameters, and the model with the best preliminary performance was selected by combining the features.

3.3.1 Side-swipe conflict

The model evaluation results of side-swipe conflict are shown in Table 2. As the number of features

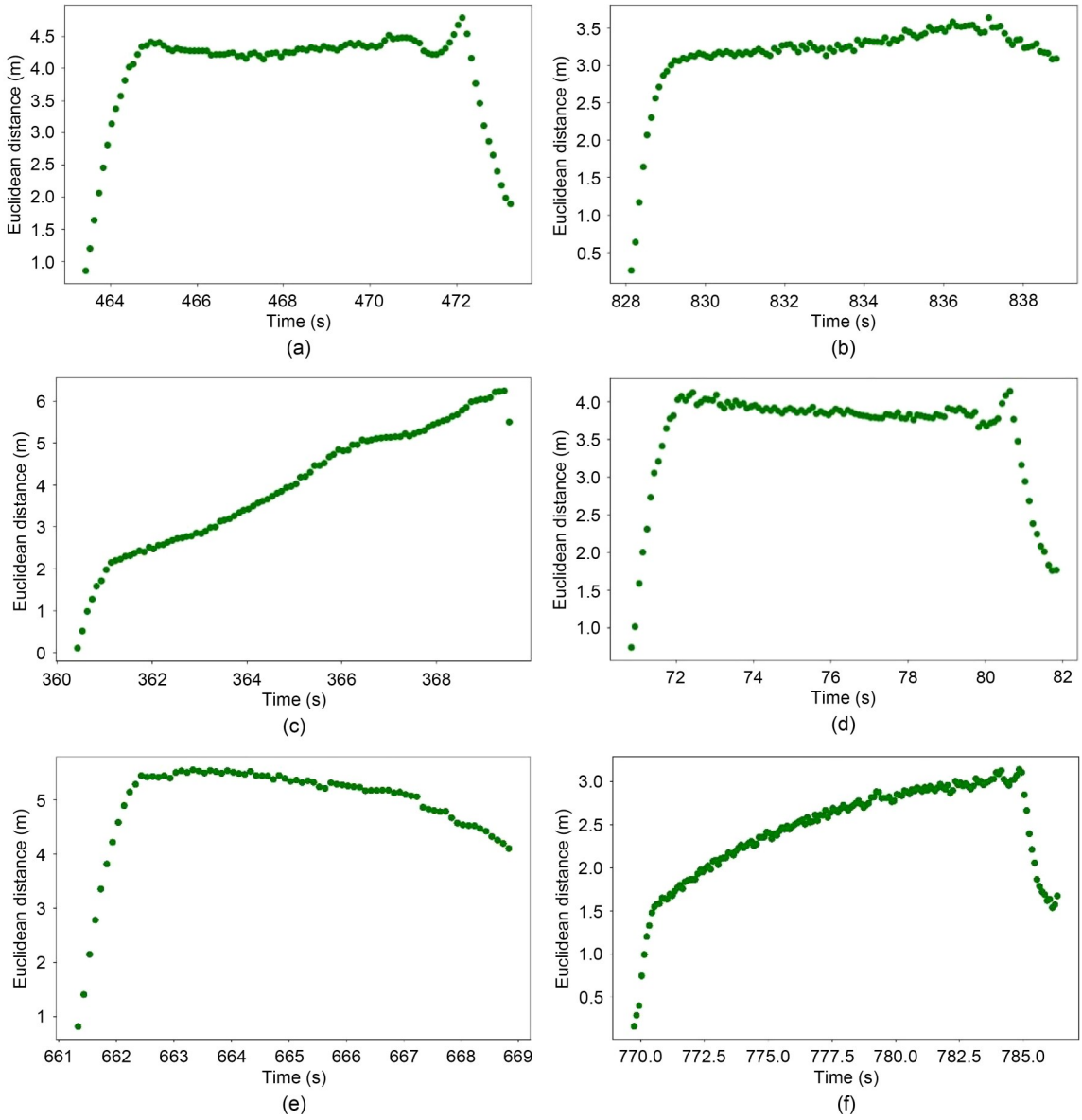

Fig. 6 Euclidean distance of reconstructed trajectory data points: (a) trajectory ID 752; (b) trajectory ID 356; (c) trajectory ID 139; (d) trajectory ID 39; (e) trajectory ID 251; (f) trajectory ID 297

increased, the performance of the models improved significantly, except for the LR model, whose performance decreased, perhaps because LR is not flexible enough in dealing with nonlinear problems. When all features were used for training, the GBDT model had the best performance, with an accuracy of 0.905, an FPR of 0.074, and an FNR of 0.149. Figs. 8a–8c show the ROC curves and AUC values of each model under different feature combinations. The AUC of the GBDT model when using all features reached 0.947. Overall, the model performance of GBDT was the best.

Then, the results of the GBDT model were analyzed for interpretability. Fig. 9 shows the SHAP value summary of the GBDT model. The features on the left are sorted by importance: those with higher speed are more important. The most important feature is the lateral speed. The higher the speed, the more likely it is to cause a side-swipe conflict. The second is the average longitudinal speed within 5 s. Faster speeds are more likely to cause conflicts. The average longitudinal acceleration within 5 s is the opposite: higher acceleration is less likely to cause conflicts. This may be because the driver judges that the road conditions

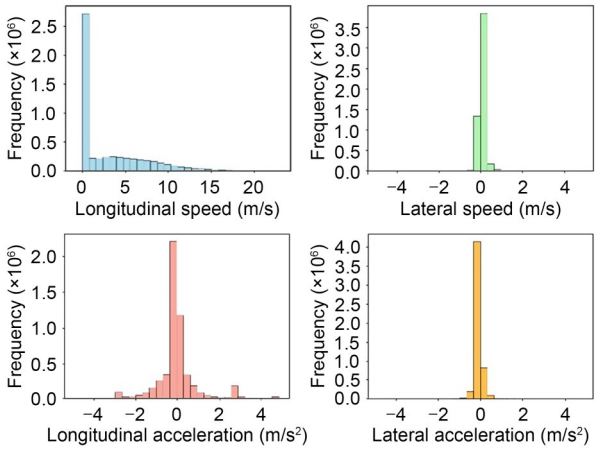

Fig. 7 Histograms of velocity and acceleration in the longitudinal and lateral directions

Table 1 Sample composition

Sample	Rear-end	Side-swipe
0	2259	573
1	1506	264

0 means no conflict and 1 means conflict

Table 2 Comparison of model performance with different feature combinations for side-swipe conflicts

Feature	Model	ACC	FPR	FNR
A	LR	0.768	0.099	0.574
	SVM	0.804	0.091	0.468
	XGBoost	0.810	0.132	0.340
	GBDT	0.780	0.165	0.362
A+B	LR	0.810	**0.066**	0.511
	SVM	0.833	0.107	0.319
	XGBoost	0.857	0.099	0.255
	GBDT	0.863	0.083	0.277
A+B+C	LR	0.798	0.074	0.532
	SVM	0.845	0.074	0.362
	XGBoost	0.869	0.083	0.255
	GBDT	**0.905**	0.074	**0.149**

The higher the ACC value and the lower the FNR and FPR values, the better the model performance. A, B, and C represent different feature sets. A represents vehicle dynamics features, while B and C are the average and standard deviation extracted from A over a 5-s time range, respectively. Detailed feature descriptions are available in Section S4 of the ESM

are safer and will maintain a higher acceleration. The SD of acceleration within 5 s measures the driver's driving style. A higher value indicates that the driver's operation is relatively unstable, which will also increase the possibility of a conflict. Overall, the impact of the first six features on conflicts is relatively important.

3.3.2 Rear-end conflict

The model evaluation results of rear-end conflict are shown in Table 3. The performance of the model using A+B+C features and A+B features did not change much, but the accuracy and FNR were better when using A+B features. When using A+B features, the best performing model was XGBoost, with an accuracy of 0.772, an FPR of 0.128, and an FNR of 0.386. Figs. 8d–8f show the ROC curves and AUC values of each model under different feature combinations. The AUC of the XGBoost model reached 0.829 when using A+B features. Overall, the model performance of XGBoost was relatively good.

Then, the interpretability of the XGBoost model results was analysed. Fig. 10 shows the SHAP value summary of the XGBoost model. Longitudinal acceleration was the most critical influencing factor in rear-end conflict, followed by factors such as the average longitudinal acceleration and longitudinal speed within 5 s. When the longitudinal acceleration was lower, conflicts were more likely to occur. This may be due to the large number of vehicles on the road, frequent vehicle interactions, and insufficient vehicle traffic, which easily leads to conflicts. When the longitudinal speed of the vehicle was low, its impact on the conflict was both positive and negative. This corresponds to two situations. When the traffic flow is smooth overall, conflicts are not likely to occur at a low speed. When the traffic flow is slow, even at a low speed, conflicts may occur easily due to increased vehicle interactions and shortened vehicle distances. This shows that it is necessary to consider multiple factors comprehensively, and confirms that when predicting conflicts, when the number of features is large, the model often predicts conflicts more accurately.

3.3.3 Conflict prediction model development

The next step was to improve the model. As shown in Section S6 of the ESM, we have clarified the importance of each feature. Now, we will present a more detailed exploration of the performance of the prediction models for side-swipe conflicts and rear-end conflicts. Starting from the most important feature, we will add features in turn to compare the changes in the model's prediction performance. The model prediction performance uses more comprehensive indicators, namely accuracy, precision, recall, F1-score, AUC, FPR, and FNR.

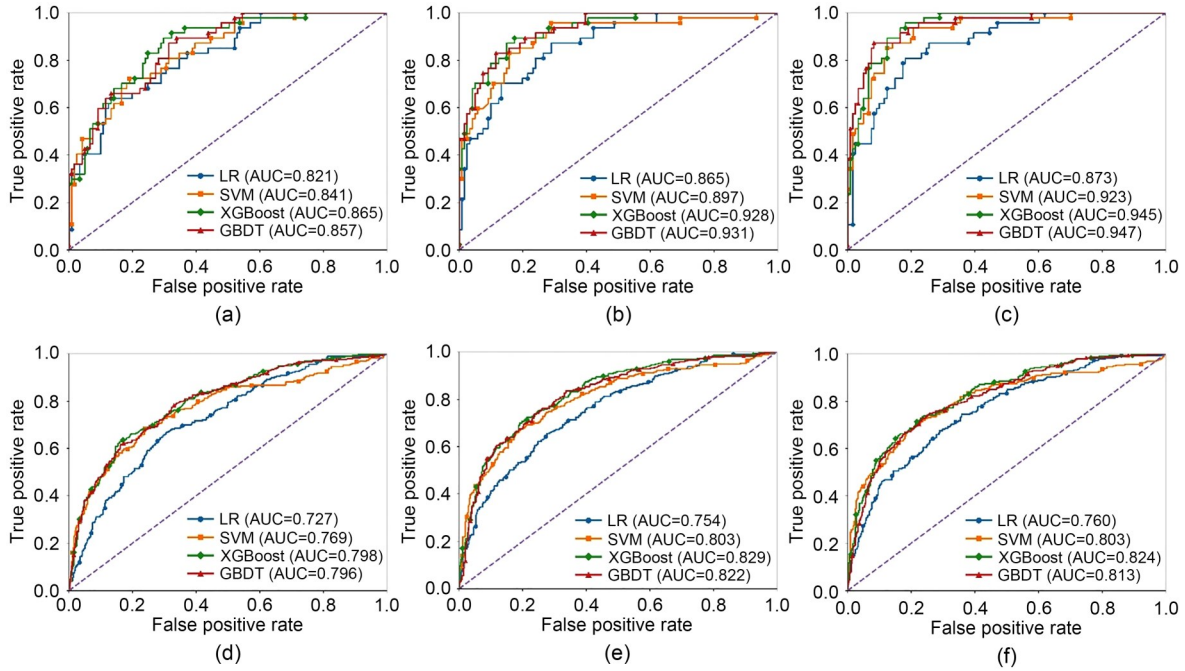

Fig. 8 ROC curves under different feature combinations: (a) side-swipe, A; (b) side-swipe, A+B; (c) side-swipe, A+B+C; (d) rear-end, A; (e) rear-end, A+B; (f) rear-end, A+B+C

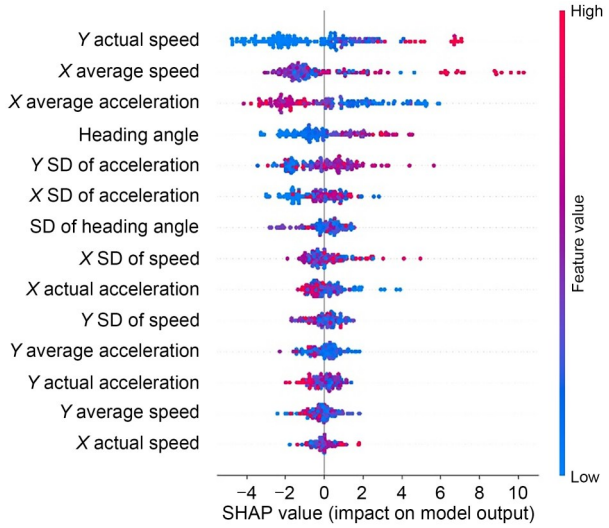

Fig. 9 Summary plot of the GBDT model with SHAP values. References to color refer to the online version of this figure

Table 3 Comparison of model performance with different feature combinations for rear-end conflicts

Feature	Model	ACC	FPR	FNR
A	LR	0.681	0.165	0.560
	SVM	0.732	0.109	0.519
	XGBoost	0.741	**0.104**	0.502
	GBDT	0.742	0.107	0.495
A+B	LR	0.696	0.215	0.444
	SVM	0.756	0.122	0.437
	XGBoost	**0.772**	0.128	0.386
	GBDT	0.765	0.146	0.375
A+B+C	LR	0.697	0.224	0.427
	SVM	0.756	0.130	0.423
	XGBoost	0.764	0.126	0.410
	GBDT	0.750	0.178	**0.362**

Evaluation indicators of the model results in Tables 2 and 3 correspond to the test part of the dataset

As the best model for predicting side-swipe conflict was GBDT when using 14 features, we added features to the GBDT model to explore the changes in model performance. The model performance became more stable when three features were added (Fig. 11a). After the 12th feature was added, the overall performance of the model peaked, with accuracy, precision, recall, F1-score, AUC, FPR, and FNR being 0.911, 0.833, 0.851, 0.842, 0.953, 0.066, and 0.149, respectively. As shown in Fig. 11b, the above steps were performed on the model with the best performance in predicting rear-end conflicts. There was a common feature in the changes in their performance indicators. After adding the third feature, the model performance indicators changed relatively smoothly, which shows that the first three features are crucial for correctly predicting collisions. The best model performance appeared

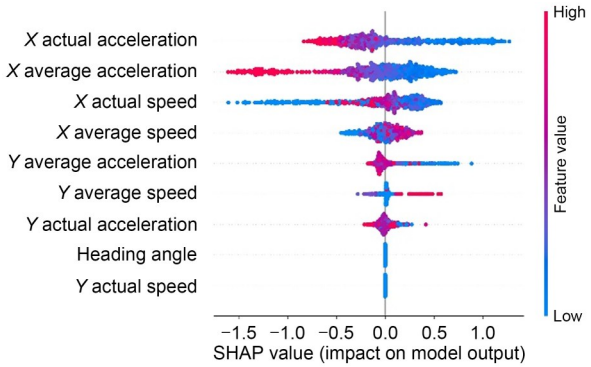

Fig. 10 Summary plot of the XGBoost model with SHAP values. References to color refer to the online version of this figure

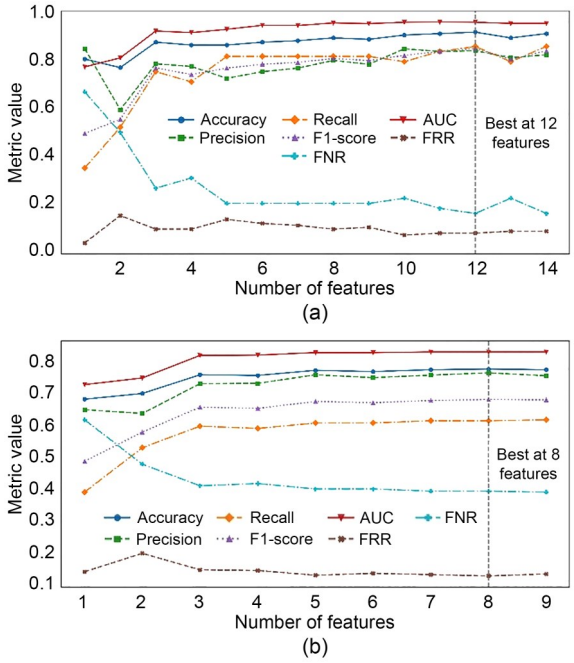

Fig. 11 Evaluation index change chart: (a) side-swipe; (b) rear-end

when the eighth feature was added, and the indicators were 0.774, 0.762, 0.611, 0.678, 0.828, 0.122, and 0.389, respectively. Section S7 of the ESM shows the parameter settings of the best model.

4 Discussion

This study was based on a vehicle trajectory dataset composed mainly of container trucks near a port area. The data were first reconstructed to improve the data quality. Then, prediction modeling was performed for two typical conflict types: the rear-end conflict and side-swipe conflict. The SHAP theory was used to analyze the interpretability of the model results and explore how each factor affected the occurrence of conflicts. Finally, by evaluating the performance of multiple machine learning models with different numbers of features, the key variables that affected the occurrence of conflicts were determined, and a prediction model with better performance was constructed.

4.1 Analysis of factors affecting conflict

Figs. 12 and 13 show the SHAP values of the top six important features for identifying the two types of collisions. For side-swipe conflicts, the most important feature is the lateral speed. This is reasonable because side-swipe conflicts usually occur in lane change scenarios. Fig. 12a shows that side-swipe conflicts are likely to occur when the lateral speed is above 0.3 m/s. This is consistent with previous research findings (Shahana and Vedagiri, 2024). Fig. 12b shows that vehicles are more likely to have conflicts when the average longitudinal speed within 5 s is low or high. Fig. 12c shows that vehicles are more likely to have conflicts when they are decelerating. They are less likely to have conflicts when they are accelerating for a long time. This corresponds to the scenarios of sudden braking and smooth traffic flow, respectively. Fig. 12d shows that higher heading angles are more likely to cause side-swipe conflicts. This finding complements previous studies that showed that higher heading angles are less likely to cause rear-end conflicts (Islam and Abdel-Aty, 2023).

For rear-end conflicts, the most important feature is the longitudinal acceleration. Fig. 13a shows that when the driver decelerates, the driver's judgment is lower than his/her safety standard. When accelerating, the driver may feel safe. The impact of the longitudinal average acceleration within 5 s on rear-end conflicts is basically the same as for the longitudinal acceleration. Fig. 13c shows that the longitudinal speed of vehicles in the range of 1–5 m/s is prone to conflict. Such a speed range shows that the overall traffic flow speed is not fast, indicating that there are many vehicles, the distance between vehicles may be small, and a certain speed is maintained, so it is more likely to cause conflicts.

The feature correlation analysis part is presented in Section S8 of the ESM.

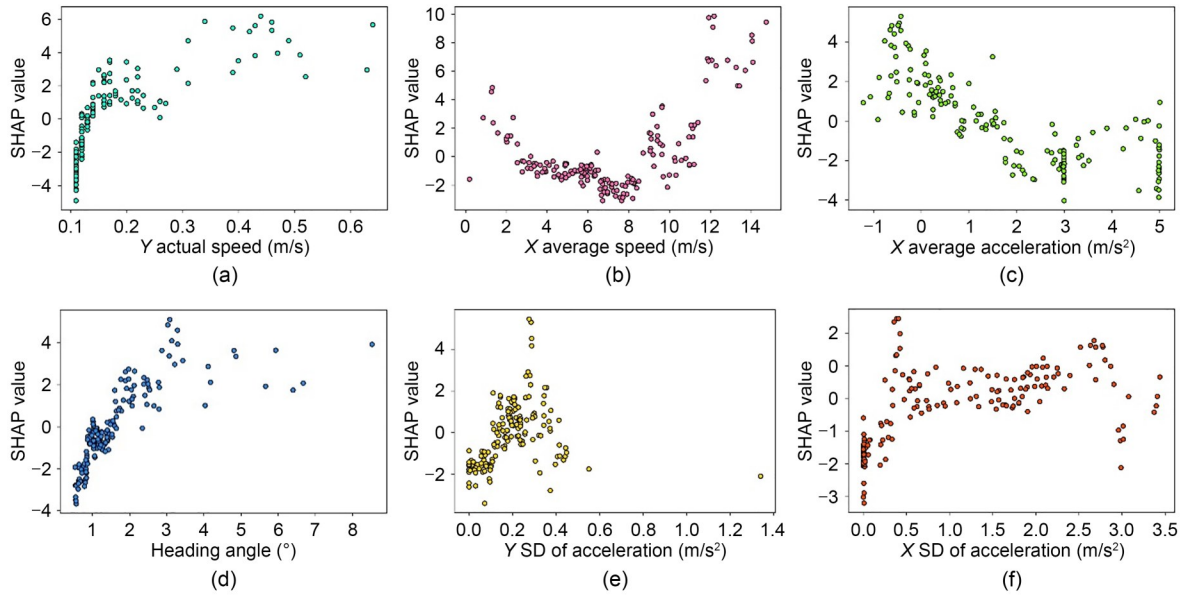

Fig. 12 SHAP values of the side-swipe feature: (a) *Y* actual speed; (b) *X* average speed; (c) *X* average acceleration; (d) heading angle; (e) *Y* SD of acceleration; (f) *X* SD of acceleration

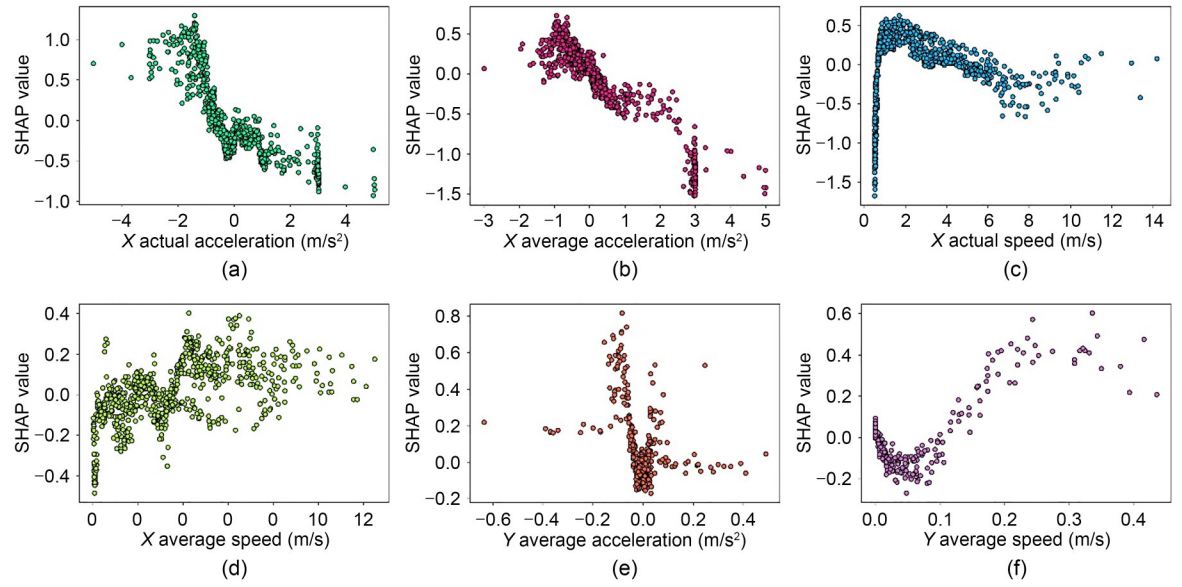

Fig. 13 SHAP values of the rear-end feature: (a) *X* actual acceleration; (b) *X* average acceleration; (c) *X* actual speed; (d) *X* average speed; (e) *Y* average acceleration; (f) *Y* average speed

4.2 Limitations

While we systematically analyzed influencing factors and constructed a rear-end conflict and side-swipe conflict prediction model based on reconstructed container truck trajectory data in a port area, several limitations remain. First, the data source is relatively limited, with strong regional and vehicle type restrictions, which may affect the model's generalization. Furthermore, we focus on the container truck traffic flow, a scenario that is relatively underrepresented in current research. Second, the model input features are based mainly on kinematic metrics and fail to incorporate multiple sources of information, such as road structure and environmental factors, making it difficult to fully characterize the conflict formation mechanism. Third, the performance of the rear-end conflict prediction model remains suboptimal, possibly due to the

complex formation mechanism of rear-end conflicts and the incomplete consideration of influencing factors. Furthermore, the model training and validation in this study are based on offline data and have not yet been tested in real traffic environments or real-time systems. Therefore, the applicability and stability of our model require further verification. Finally, while methods such as SHAP were introduced for feature interpretation, SHAP analysis results may be affected by inter-feature correlations and model structure, resulting in limitations in interpreting causal relationships. Subsequent research could include the following aspects: at the data level, trajectory data of different regions, vehicle types, and time periods could be expanded to improve the generalization of the model; at the feature level, multi-source information, such as road geometry, traffic flow density, and meteorological conditions, could be integrated to characterize the conflict mechanism more comprehensively; at the method level, multi-scale time series modeling and model integration could be explored and verified in real traffic or simulation environments; at the same time, explainable artificial intelligence and traffic safety mechanisms could be combined to improve the stability, credibility, and generalizability of the model.

5 Conclusions

This study reconstructed the trajectory data of vehicles, mainly container trucks, near a port area to obtain a high-resolution and high-precision vehicle trajectory dataset. Then, based on the coordinate format output by YOLOv8, a 2D-TTC was developed to identify side-swipe conflicts. Samples of two types of conflicts, side-swipe and rear-end conflicts, were collected for container truck traffic flow. A machine learning model and SHAP theory were used to analyze the influencing factors, and a model for predicting these two conflicts was developed. The main conclusions of this study are as follows:

(1) Compared with the original data, after trajectory reconstruction, the trajectory and its speed, acceleration, and jerk become more reasonable, which is in line with the actual vehicle driving conditions. The video dataset shot by drones has the problem of data accuracy, and the trajectory reconstruction method solves this problem well.

(2) Considering the interaction of vehicles in 2D space, the developed 2D-TTC can well identify side-swipe conflicts. Higher lateral speed and average longitudinal speed within 5 s are more likely to cause side-swipe conflicts, and lower average acceleration within 5 s is also more likely to cause conflicts. The GBDT model with 12 features was finally selected to achieve the best performance in identifying side-swipe conflicts, with an accuracy of 0.911 and an AUC of 0.953.

(3) The most important features affecting rear-end conflicts are longitudinal acceleration and average acceleration within 5 s. When these two values are low, rear-end conflicts are more likely to occur. Finally, the XGBoost model with eight features was selected, which achieved the best performance in identifying rear-end conflicts, with an accuracy of 0.774 and an AUC of 0.828.

Acknowledgments

This work is supported by the Program of Humanities and Social Science of the Education Ministry of China (No. 24YJA630013), the Ningbo Natural Science Foundation of China (No. 2024J125), and the "Innovation Yongjiang 2035" Key R&D Programme (No. 2024H032), China.

Author contributions

Zhihao ZHU: conceptualization, methodology, and writing–original draft. Hexuan LIU: investigation, validation, data curation, and formal analysis. Rongjun CHENG: writing–review & editing and supervision.

Conflict of interest

The authors declare that they have no known competing financial interests or personal relationships that could have appeared to influence the work reported in this paper.

References

Ahn S, Vadlamani S, Laval J, 2013. A method to account for non-steady state conditions in measuring traffic hysteresis. *Transportation Research Part C: Emerging Technologies*, 34:138-147. https://doi.org/10.1016/j.trc.2011.05.020

Andersson JAE, Gillis J, Horn G, et al., 2019. CasADi: a software framework for nonlinear optimization and optimal control. *Mathematical Programming Computation*, 11(1): 1-36. https://doi.org/10.1007/s12532-018-0139-4

Barmpounakis E, Geroliminis N, 2020. On the new era of urban traffic monitoring with massive drone data: the pneuma large-scale field experiment. *Transportation Research Part C: Emerging Technologies*, 111:50-71.

https://doi.org/10.1016/j.trc.2019.11.023

Bradley AP, 1997. The use of the area under the roc curve in the evaluation of machine learning algorithms. *Pattern Recognition*, 30(7):1145-1159. https://doi.org/10.1016/S0031-3203(96)00142-2

Chen AY, Chiu YL, Hsieh MH, et al., 2020. Conflict analytics through the vehicle safety space in mixed traffic flows using UAV image sequences. *Transportation Research Part C: Emerging Technologies*, 119:102744. https://doi.org/10.1016/j.trc.2020.102744

Chen TQ, Guestrin C, 2016. XGBoost: a scalable tree boosting system. Proceedings of the 22nd ACM SIGKDD International Conference on Knowledge Discovery and Data Mining, p.785-794. https://doi.org/10.1145/2939672.2939785

Friedman JH, 2001. Greedy function approximation: a gradient boosting machine. *The Annals of Statistics*, 29(5): 1189-1232. https://doi.org/10.1214/AOS/1013203451

Gu X, Abdel-Aty M, Xiang QJ, et al., 2019. Utilizing UAV video data for in-depth analysis of drivers' crash risk at interchange merging areas. *Accident Analysis & Prevention*, 123:159-169. https://doi.org/10.1016/j.aap.2018.11.010

Hayward JC, 1972. Near miss determination through use of a scale of danger. *Highway Research Record*, 384:24-34.

He JC, Peng B, Feng ZY, et al., 2024. A Gaussian mixture unscented Rauch–Tung–Striebel smoothing framework for trajectory reconstruction. *IEEE Transactions on Industrial Informatics*, 20(5):7481-7491. https://doi.org/10.1109/TII.2024.3360478

Hou J, List GF, Guo XC, 2014. New algorithms for computing the time-to-collision in freeway traffic simulation models. *Computational Intelligence and Neuroscience*, 2014(1): 761047. https://doi.org/10.1155/2014/761047

Hou KN, Zou J, Zheng FF, et al., 2024. On the precise quantification of the impact of a single discretionary lane change on surrounding traffic. arXiv:2407.18557. https://doi.org/10.48550/arXiv.2407.18557

Hu XW, Zheng ZD, Chen DJ, et al., 2022. Processing, assessing, and enhancing the Waymo autonomous vehicle open dataset for driving behavior research. *Transportation Research Part C: Emerging Technologies*, 134:103490. https://doi.org/10.1016/j.trc.2021.103490

Hu YP, Li Y, Huang HL, et al., 2022. A high-resolution trajectory data driven method for real-time evaluation of traffic safety. *Accident Analysis & Prevention*, 165:106503. https://doi.org/10.1016/j.aap.2021.106503

Islam Z, Abdel-Aty M, 2023. Traffic conflict prediction using connected vehicle data. *Analytic Methods in Accident Research*, 39:100275. https://doi.org/10.1016/j.amar.2023.100275

Jansen RJ, Varotto SF, 2022. Caught in the blind spot of a truck: a choice model on driver glance behavior towards cyclists at intersections. *Accident Analysis & Prevention*, 174:106759. https://doi.org/10.1016/j.aap.2022.106759

Ji Q, Lyu H, Yang H, et al., 2023. Bifurcation control of solid angle car-following model through a time-delay feedback method. *Journal of Zhejiang University-SCIENCE A*, 24(9):828-840. https://doi.org/10.1631/jzus.A2300026

Jiao YR, Calvert SC, van Cranenburgh S, et al., 2025. A unified probabilistic approach to traffic conflict detection. *Analytic Methods in Accident Research*, 45:100369. https://doi.org/10.1016/j.amar.2024.100369

Katrakazas C, Quddus M, Chen WH, 2018. A simulation study of predicting real-time conflict-prone traffic conditions. *IEEE Transactions on Intelligent Transportation Systems*, 19(10):3196-3207. https://doi.org/10.1109/TITS.2017.2769158

Krajewski R, Bock J, Kloeker L, et al., 2018. The highD dataset: a drone dataset of naturalistic vehicle trajectories on German highways for validation of highly automated driving systems. 2018 21st International Conference on Intelligent Transportation Systems (ITSC), p.2118-2125. https://doi.org/10.1109/ITSC.2018.8569552

Li GF, Yang YF, Li S, et al., 2022. Decision making of autonomous vehicles in lane change scenarios: deep reinforcement learning approaches with risk awareness. *Transportation Research Part C: Emerging Technologies*, 134: 103452. https://doi.org/10.1016/j.trc.2021.103452

Li JQ, Cheng RJ, 2025. A real-time adaptive signal control method for multi-intersections in mixed connected vehicle environments. *Journal of Zhejiang University-SCIENCE A*, 26(8):801-810. https://doi.org/10.1631/jzus.A2400488

Li JQ, Wang XS, Yang XH, et al., 2024. Analyzing freeway safety influencing factors using the CatBoost model and interpretable machine-learning framework, SHAP. *Transportation Research Record*, 2678(7):563-574. https://doi.org/10.1177/03611981231208903

Li LY, Lyu H, Wang T, et al., 2024. STdi4DMPC: distributed model predictive control for connected and automated truck platoon with mixed traffic flow based on spatio-temporal trajectory prediction. *IEEE Transactions on Vehicular Technology*, 73(10):14563-14579. https://doi.org/10.1109/TVT.2024.3412992

Li P, Abdel-Aty M, Cai Q, et al., 2020. The application of novel connected vehicles emulated data on real-time crash potential prediction for arterials. *Accident Analysis & Prevention*, 144:105658. https://doi.org/10.1016/j.aap.2020.105658

Liu MQ, Zhao J, Hoogendoorn S, et al., 2022. A single-layer approach for joint optimization of traffic signals and cooperative vehicle trajectories at isolated intersections. *Transportation Research Part C: Emerging Technologies*, 134:103459. https://doi.org/10.1016/j.trc.2021.103459

Lundberg SM, Lee SI, 2017. A unified approach to interpreting model predictions. Proceedings of the 31st International Conference on Neural Information Processing Systems, p.4768-4777.

Martinez JJ, Canudas-de-Wit C, 2007. A safe longitudinal control for adaptive cruise control and stop-and-go scenarios. *IEEE Transactions on Control Systems Technology*, 15(2): 246-258.
https://doi.org/10.1109/TCST.2006.886432

Mohammadian S, Haque MM, Zheng ZD, et al., 2021. Integrating safety into the fundamental relations of freeway traffic flows: a conflict-based safety assessment framework. *Analytic Methods in Accident Research*, 32:100187.
https://doi.org/10.1016/j.amar.2021.100187

Montanino M, Punzo V, 2015. Trajectory data reconstruction and simulation-based validation against macroscopic traffic patterns. *Transportation Research Part B: Methodological*, 80:82-106.
https://doi.org/10.1016/j.trb.2015.06.010

Orsini F, Gecchele G, Rossi R, et al., 2021. A conflict-based approach for real-time road safety analysis: comparative evaluation with crash-based models. *Accident Analysis & Prevention*, 161:106382.
https://doi.org/10.1016/j.aap.2021.106382

Ouyang PY, Guo YY, Liu P, et al., 2025. An approach for evaluating traffic safety of expressway weaving segments: investigating risk patterns of lane-changing conflicts. *Journal of Transportation Safety & Security*, 17(2):125-157.
https://doi.org/10.1080/19439962.2024.2372292

Peng ZP, Zuo JP, Ji H, et al., 2024. A comparative analysis of risk factors in taxi-related crashes using XGBoost and SHAP. *International Journal of Injury Control and Safety Promotion*, 31(3):508-520.
https://doi.org/10.1080/17457300.2024.2349555

Rafati Fard M, Shariat Mohaymany A, Shahri M, 2017. A new methodology for vehicle trajectory reconstruction based on wavelet analysis. *Transportation Research Part C: Emerging Technologies*, 74:150-167.
https://doi.org/10.1016/j.trc.2016.11.010

Ribeiro MT, Singh S, Guestrin C, 2016. "Why should I trust you?": explaining the predictions of any classifier. Proceedings of the 22nd ACM SIGKDD International Conference on Knowledge Discovery and Data Mining, p.1135-1144.
https://doi.org/10.1145/2939672.2939778

Safavian SR, Landgrebe D, 1991. A survey of decision tree classifier methodology. *IEEE Transactions on Systems, Man, and Cybernetics*, 21(3):660-674.
https://doi.org/10.1109/21.97458

Shahana A, Vedagiri P, 2024. Developing rear-end and sideswipe conflict prediction models for urban signalized intersections under disordered traffic conditions. *IATSS Research*, 48(1):1-13.
https://doi.org/10.1016/j.iatssr.2023.12.004

Shawky M, Alsobky A, Al Sobky A, et al., 2023. Traffic safety assessment for roundabout intersections using drone photography and conflict technique. *Ain Shams Engineering Journal*, 14(6):102115.
https://doi.org/10.1016/j.asej.2023.102115

Thiemann C, Treiber M, Kesting A, 2008. Estimating acceleration and lane-changing dynamics from next generation simulation trajectory data. *Transportation Research Record*, 2088(1):90-101.
https://doi.org/10.3141/2088-10

Tian JF, Zhang HM, Treiber M, et al., 2019. On the role of speed adaptation and spacing indifference in traffic instability: evidence from car-following experiments and its stochastic model. *Transportation Research Part B: Methodological*, 129:334-350.
https://doi.org/10.1016/j.trb.2019.09.014

Tian ZQ, Chen FC, Ma SQ, et al., 2024. Analysis of the severity of heavy truck traffic accidents under different road conditions. *Applied Sciences*, 14(22):10751.
https://doi.org/10.3390/app142210751

Vapnik VN, 1995. The Nature of Statistical Learning Theory. Springer, New York, USA.

Venthuruthiyil SP, Chunchu M, 2022. Anticipated collision time (ACT): a two-dimensional surrogate safety indicator for trajectory-based proactive safety assessment. *Transportation Research Part C: Emerging Technologies*, 139: 103655.
https://doi.org/10.1016/j.trc.2022.103655

Wächter A, Biegler LT, 2006. On the implementation of an interior-point filter line-search algorithm for large-scale nonlinear programming. *Mathematical Programming*, 106(1): 25-57.
https://doi.org/10.1007/s10107-004-0559-y

Wang C, Xu CC, Dai YL, 2019. A crash prediction method based on bivariate extreme value theory and video-based vehicle trajectory data. *Accident Analysis & Prevention*, 123:365-373.
https://doi.org/10.1016/j.aap.2018.12.013

Ward JR, Agamennoni G, Worrall S, et al., 2015. Extending time to collision for probabilistic reasoning in general traffic scenarios. *Transportation Research Part C: Emerging Technologies*, 51:66-82.
https://doi.org/10.1016/j.trc.2014.11.002

Wu FY, Stern RE, Cui SM, et al., 2019. Tracking vehicle trajectories and fuel rates in phantom traffic jams: methodology and data. *Transportation Research Part C: Emerging Technologies*, 99:82-109.
https://doi.org/10.1016/j.trc.2018.12.012

Xie K, Yang D, Ozbay K, et al., 2019. Use of real-world connected vehicle data in identifying high-risk locations based on a new surrogate safety measure. *Accident Analysis & Prevention*, 125:311-319.
https://doi.org/10.1016/j.aap.2018.07.002

Xing L, He J, Abdel-Aty M, et al., 2019. Examining traffic conflicts of up Stream toll plaza area using vehicles' trajectory data. *Accident Analysis & Prevention*, 125:174-187.
https://doi.org/10.1016/j.aap.2019.01.034

Xing L, He J, Li Y, et al., 2020. Comparison of different models for evaluating vehicle collision risks at upstream diverging area of toll plaza. *Accident Analysis & Prevention*, 135:105343.
https://doi.org/10.1016/j.aap.2019.105343

Yao RY, Zeng WL, Chen YH, et al., 2021. A deep learning

framework for modelling left-turning vehicle behaviour considering diagonal-crossing motorcycle conflicts at mixed-flow intersections. *Transportation Research Part C: Emerging Technologies*, 132:103415. https://doi.org/10.1016/j.trc.2021.103415

Yuan C, Li Y, Huang HL, et al., 2022. Using traffic flow characteristics to predict real-time conflict risk: a novel method for trajectory data analysis. *Analytic Methods in Accident Research*, 35:100217. https://doi.org/10.1016/j.amar.2022.100217

Zaki MH, Sayed T, Shaaban K, 2014. Use of drivers' jerk profiles in computer vision-based traffic safety evaluations. *Transportation Research Record*, 2434(1):103-112. https://doi.org/10.3141/2434-13

Zhao J, Ma RM, Wang M, 2024a. A behaviourally underpinned approach for two-dimensional vehicular trajectory reconstruction with constrained optimal control. *Transportation Research Part C: Emerging Technologies*, 159:104489. https://doi.org/10.1016/j.trc.2024.104489

Zhao J, Yang XL, Zhang C, 2024b. Vehicle trajectory reconstruction for intersections: an integrated wavelet transform and Savitzky-Golay filter approach. *Transportmetrica A: Transport Science*, 20(2):2163207. https://doi.org/10.1080/23249935.2022.2163207

Zheng L, Hu ZL, Sayed T, 2023. Traffic conflict prediction at signal cycle level using Bayesian optimized machine learning approaches. *Transportation Research Record*, 2677(5):183-195. https://doi.org/10.1177/03611981221128812

Zheng O, Abdel-Aty M, Yue LSS, et al., 2024. CitySim: a drone-based vehicle trajectory dataset for safety-oriented research and digital twins. *Transportation Research Record: Journal of the Transportation Research Board*, 2678(4):606-621. https://doi.org/10.1177/03611981231185768

Zhou MF, Qu XB, Li XP, 2017. A recurrent neural network based microscopic car following model to predict traffic oscillation. *Transportation Research Part C: Emerging Technologies*, 84:245-264. https://doi.org/10.1016/j.trc.2017.08.027

Zhu ZH, Meng Y, Cheng RJ, 2025. Container truck high-risk events prediction and its influencing factors analyses based on trajectory data. *Systems*, 13(5):326. https://doi.org/10.3390/systems13050326

Electronic supplementary materials

Sections S1–S8, Eqs. (S1)–(S7)